

A Method to Estimate Aerosol Load on a Pixel-by-Pixel Basis Using Airborne Hyperspectral Sensors: A Case Study over Santa Monica, California

Eyal Ben-Dor¹ and Bruce Kindel²

¹ The Remote Sensing and GIS Laboratories, Department of Geography
Tel-Aviv University, Israel

² Center for the Study of Earth from Space (CSES)
Cooperative Institute for Research in Environment Sciences (CIRES)
University of Colorado

INTRODUCTION

The advantage of hyperspectral technology is the ability to record small and narrow spectral features of both terrestrial and atmospheric components. Whereas terrestrial applications gained much attention and progress by many researchers, utilization of the atmospheric signals has not yet developed beyond the water vapor content current estimation. This is mainly due to the limited information the available hyperspectral (HRS) scanners can provide with reasonable signal quality as to the gas's spectral absorption. Extensive studies from HRS perspective and methodologies to depict water vapor content on a pixel-by-pixel basis have been developed by many researchers (e.g., Gao et al., 1993b, Richter, 2004). Knowledge of the water vapor content on a pixel-by-pixel basis enables better atmospheric correction and provides sharper HRS reflectance data. A recent work by Green (2001) showed also that the CO₂ content can be estimated using the absorption peaks at around 2.005 μm and 2.055 μm on a pixel basis. Using the CO₂ absorption features from an AVIRIS cube enabled Green (2001) to present good agreement between the topography and the CO₂ content over California's San Gabriel Mountains.

In flat terrain, excluding water vapor, all other atmospheric attenuations are considered to be constant. Whereas this consideration is mostly true for well-mixed gases such as O₂, CO₂ and O₃ it may not be the case for the aerosol load. Smoke, local dust or point particle emission to the air may hamper correct reflectance retrieval regarding the area in question. Furthermore, non-visible dust particles that may not be monitored spatially still can deteriorate air and life qualities. Determining the aerosols content on a pixel-by-pixel perspective using airborne data only (as done with the water vapor estimation) is still unavailable to the best of our knowledge. Ben-Dor et al. (1994) had shown that thin cirrus clouds can be spatially monitored in AVIRIS images using the oxygen peak at 0.76 μm and concluded that scattering effects of the non-visible ice particles contribute to the oxygen absorption response and affect its spectral signal. Based on this finding, and based on the understanding that AVIRIS data today is much better in its signal quality than the 1994 data, we propose in this study to examine a possible method at point estimation of aerosol load over an urban environment.

MATERIALS AND METHODS

In order to examine this idea we first generated a synthetic AVIRIS radiance scene composed of vegetation and urban materials with constant water vapor, constant concentration of other gases (O_3 , O_2 and CO_2) and varying aerosol load. The synthetic AVIRIS cube was generated using the atmospheric radiative transfer code MODTRAN 4.0 (Berk et al., 1999). The code was run 100 times, corresponding to 100 aerosol load (visibility of 0–100 km) with water vapor content of 1.1 cm (estimated from authentic AVIRIS data of *Santa Monica 2000*). In order to generate the inputs for predicting the at-sensor radiance for each aerosol load, the code was run three times with constant albedos of 0.0 (the path radiance term), 0.5 and 1.0. Using these results, the two-way transmittance, path radiance, and spherical albedo were generated. With the addition of the surface reflectance and exoatmospheric solar spectrum, the at-sensor radiance was predicted. The solar geometry was chosen to replicate an “average” imaging spectrometer data collection, run with a solar zenith angle identical for an authentic AVIRIS scene selected later for further study. The MODTRAN code was set to the “mid-latitude summer” model, a constant surface elevation (0 km), changing visibility, constant water vapor level of 1.1 cm and a CO_2 mixing ratio of 360 ppm from altitudes of 20 km. The runs were performed with MODTRAN's two-stream DISORT and correlated-k algorithm ASDS (Ben-Dor et al., 2004).

The surface spectral information input to the synthetic data sets was obtained from two ASD-FR field spectra of urban and vegetation environments, acquired in typical urban areas (vegetation: mixture of grass and trees canopy; urban: mixture of concrete, asphalt, soil and dry wood). The vegetation and urban spectra were “mixed” linearly in 1% increments. The MODTRAN and ASD-FR spectra were convolved to an actual AVIRIS 2000 wavelength file (band centers and FWHM). The synthetic cube was constructed as follows: the 100 samples across the image are the 100 aerosol load values; sample 1 contains 0-km visibility and sample 100 contains 100-km visibility. The top line consists of 100% vegetation, and the bottom line of 99% urban (see Figure 1). The data were scaled by 10,000 and then converted to integer, and finally scaled by the AVIRIS scaling factors. Previous to this, all calculations were performed as floating point.

The authentic AVIRIS data that was selected for this study was of Santa Monica acquired on June 6, 2000 from an altitude of 20 km. The image was atmospherically corrected using ACORN code to yield an apparent reflectance cube and a water vapor image. Whereas the average water value of the scene (1.1 cm) was used in the synthetic data, the apparent reflectance image was processed to yield a “quick view” of the land use areas, as will be discussed later.

RESULT AND DISCUSSION

Ben-Dor et al. (1994) had shown that applying the parameter $\ln(A/R)$ to each pixel in the AVIRIS radiance/sun images (where A is the absorption of the oxygen peak at $0.760 \mu m$ and R is the reflectance at $0.760 \mu m$ if no oxygen absorption appears, i.e., the value on the continuum line of the oxygen peak) can extract a thin cirrus cloud image identified at $1.38 \mu m$ (A wavelength suggested by Gao et al. (1993) as a cirrus clouds marker in MODIS). Based on these findings we suggest using this parameter to further account for the aerosol loading on a pixel-by-pixel basis. Taking this challenge, we calculated the $\ln(A/R)$ over the synthetic image and segregated the calculated values to represent pure vegetation (100%), mixed vegetation-urban (50%) and pure urban pixels (100%).

Figure 2 shows the $\ln(A/R)$ values over these targets as a function of the visibility. As seen, a similar asymptotic trend was obtained for the three targets with an offset going from

urban (low) to vegetation (high) targets. This offset is due to the spectral contribution of each target across the oxygen absorption peak and can be termed as the “albedo interference.” The overall shape of the graphs presented in Figure 2 is based on the contribution of particle scattering to the oxygen absorption response at 0.760 μm . In reality, the oxygen, as a well-mixed gas, should provide a homogenous $\ln(A/R)$ image. Any variation from homogeneity may be related majorly to aerosol scattering appearance and/or minorly to the targets albedo variations. To reduce the albedo effect we used a look-up-table that was generated directly from Figure 2 and was set to represent 100% vegetation, 50% vegetation+50% urban and 100% urban materials. Parallel to that we used the authentic AVIRIS image, which was first processed to remove the atmospheric attenuations by ACORN (2001) software (with a single visibility value of 25 km). The “atmospherically corrected” image was then interoperated using the SAM classifier for two end members, namely vegetation and urban material that were taken from the image. Each pixel in the authentic scene was characterized either as vegetation, urban or their mixture (excluding outliers), and then was classified to one of the three groups (100% vegetation(a), 50% vegetation + 50% urban(b) and 100% urban(c)). The $\ln(A/R)$ was calculated from the authentic AVIRIS radiance and then, was converted to present the visibility image. This was done by applying to each $\ln(A/R)$ calculated pixel a proper look-up-table that converts the data into visibility. The proper look-up-table for that purpose was selected based on the SAM classification and Figure 2. Adding all pixels together provided the visibility (albedo corrected) image of the area. Figure 3 shows a natural RGB image (a) of a Santa Monica, California, area side by side to the visibility image (b) of the same area, as was generated according to the process described above.

EVALUATION OF THE RESULTS AND FURTHER WORK

From Figure 2 it is seen that beyond ~ 30 km visibility the $\ln(A/R)$ values do not significantly change with increasing visibility. This suggests that a traditional visibility estimation, as done by an observer (for atmospherically rectifying remote sensing images), cannot be that precise; therefore, rough estimation is sufficient (e.g., 30 km or 40 km may provide similar $\ln(A/R)$ values). Nevertheless, on hazy days or over dusty areas, the visibility may be fairly low. In this regard, the $\ln(A/R)$ parameter is significantly affected by the aerosols load and can be used to precisely assess the correct visibility values over those pixels.

The histogram of the visibility image is given in Figure 4. It shows that an average of 30 km represents the entire scene. Several pixels however are characterized with lower visibility and can be seen in the image as darker tone areas (Figure 3b). The areas with low visibilities are those suspected to hold high aerosols load. From the image it is postulated that the lowest aerosol pixels are concentrated along a main strip (A in Figure 3b). As we have no ground truth data to validate this observation, we can only speculate that other areas are relatively contaminated with more fine particles in the air than the other areas. However, it should be remembered that this speculation has not been validated yet and more study in this direction has to be applied. Although this limitation may hamper a concrete conclusion, we believe that the suggested method has a favorable potential in depicting aerosol load on a pixel-by-pixel basis.

SUMMARY AND CONCLUSION

We presented here an idea and a first analytical step on how to account for the aerosol load on a pixel-by-pixel basis. The oxygen peak was used as a marker to pick the scattering effect of the aerosols and a look-up-table was set to reduce albedo effects of atmospherically

studied components (aerosols and oxygen). The visibility image generated based on the suggested method showed a reasonable distribution over Santa Monica, California. Nevertheless, a proper validation process that can make such a method more concrete is still missing. More work in this direction is required and a combined research which will use low visibility data and ground truth information is strongly advised. Needless to say, only imaging spectrometry can provide such feasibility, and for that purpose, high quality data (e.g., AVIRIS) is a must.

REFERENCE

- ACORN™, 2001, Atmospheric Correction Now. Analytical Imaging and Geophysics LLC, Version 3.12
- Ben-Dor, E., A.F.H. Goetz, and A.T. Shapiro, 1994, Estimation of cirrus cloud and aerosol scattering in hyperspectral image data, *Proceedings of the International Symposium on Spectral Sensing Research*, 2:582–593, San Diego, California, USA
- Ben-Dor, E., B. Kindel, and A.F.H. Goetz, 2004, Quality Assessment of Several Methods to Recover Surface Reflectance I using Synthetic Imaging Spectroscopy (IS) Data, *Remote Sensing of Environment* 90: 389–404
- Berk, A., G.P. Anderson, L.S. Bernstein, P.K. Acharya, H. Dothe, M.W. Matthew, S.M. Adler-Golden, J.H. Chetwynd, Jr., S.C. Richtsmeier, B. Pukall, C.L. Allred, L.S. Jeong, and M.L. Hoke, 1999, [MODTRAN 4 Radiative Transfer Modeling for Atmospheric Correction](#) *Summaries of the Eighth JPL Airborne Earth Science Workshop* JPL-Pub 99-17: 23–31
- Gao, B.C., A.F.H. Goetz, and W.J. Wiscombe, 1993, Cirrus cloud detection from airborne imaging spectrometer data using the 1.38 mm water vapor band, *Geophysical Research Letters* 20(4): 301–304
- Gao, B.C., K.B. Heidebrecht, and A.F.H. Goetz, 1993, Derivation of Scaled Surface Reflectance from AVIRIS Data, *Remote Sens. Environ.* 44, 145–163
- Green, R.O., 2001, Measuring the Spectral Expression of Carbon Dioxide in the Solar Reflected Spectrum with AVIRIS, *Proceedings of the 10th JPL Airborne Earth Science Workshop*, JPL Publication 02-1, Jet Propulsion Laboratory, Pasadena, California, 181–192
- Richter, R., Atmospheric/Topographic Correction for Airborne Imagery (ATCOR-4), DLR report DLR-IB 565-02/04, Wesling, Germany

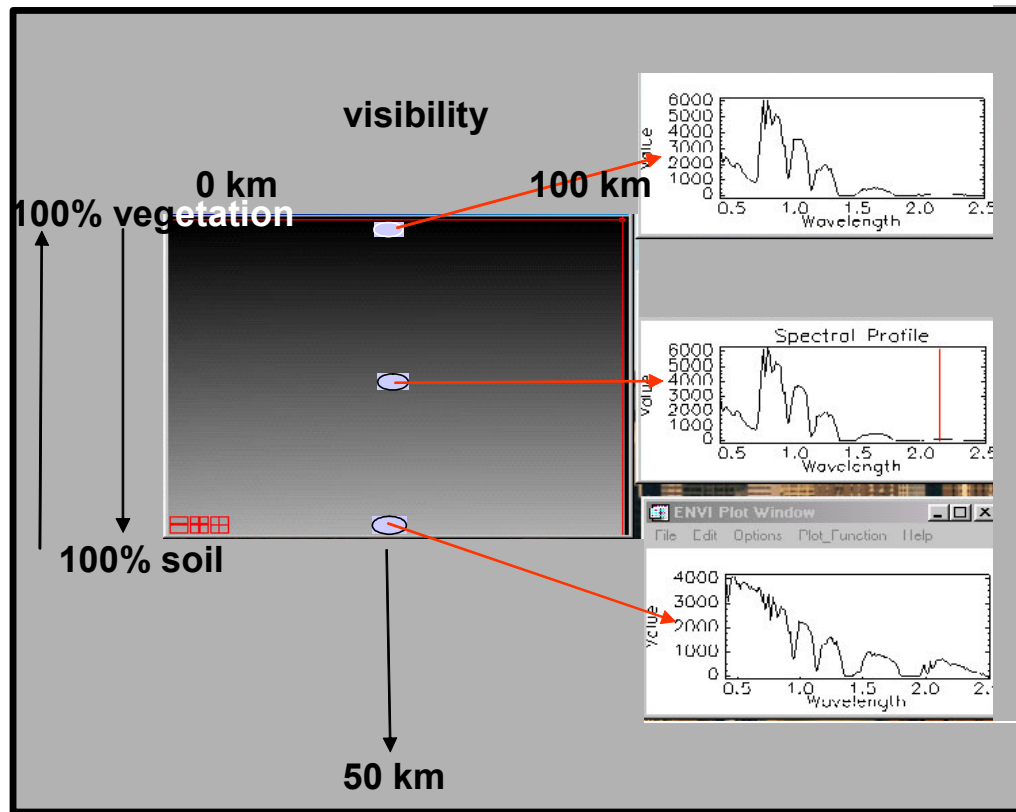


Figure 1: The synthetic radiance image and the spatial distribution of the visibility (X axis) and the urban and vegetation cover (Y axis)

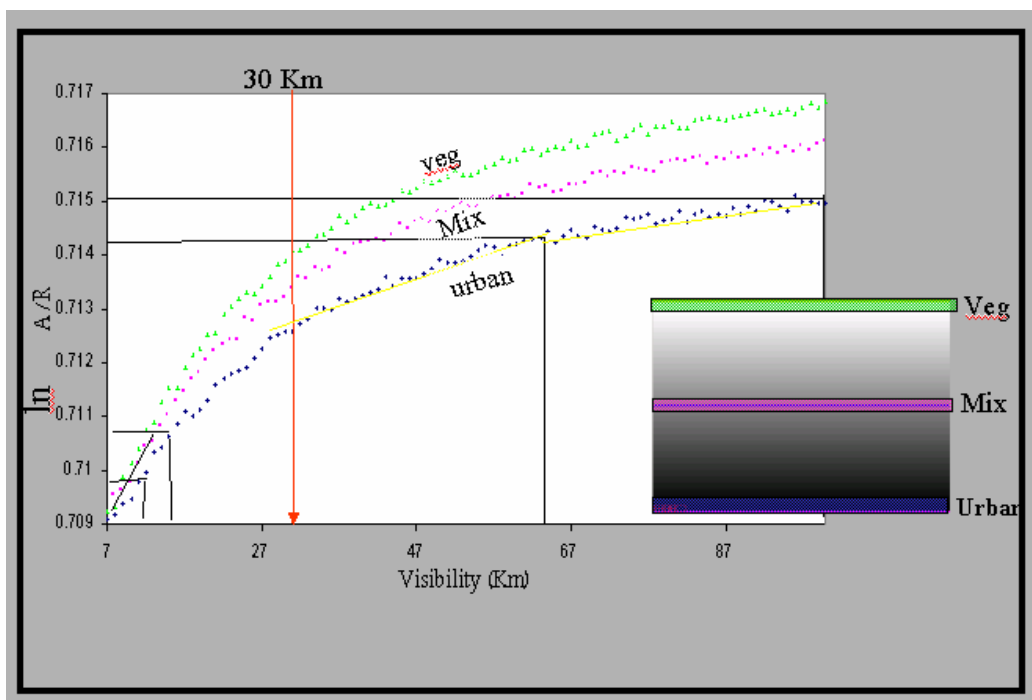


Figure 2: The $\ln(A/R)$ at $0.760 \mu\text{m}$ as a function of the visibility in the synthetic image for 100% the vegetation, 50% vegetation + 50% urban and 100% urban targets

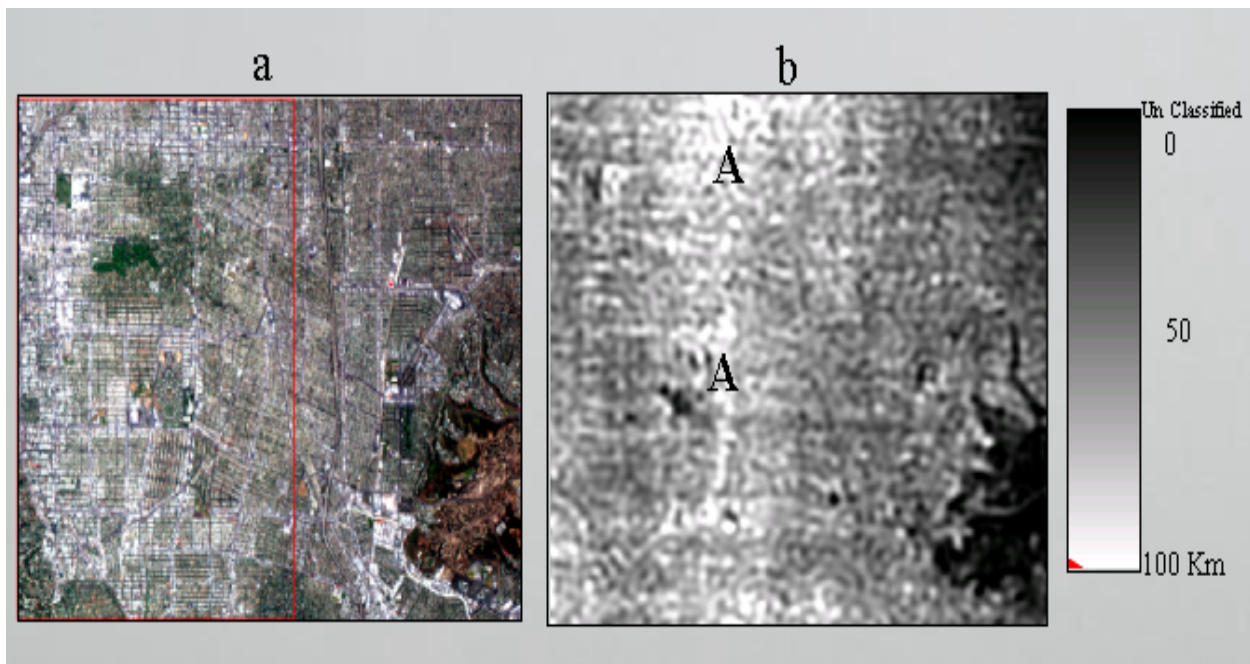


Figure 3: A natural color view of the area under study (a) and its visibility image generated according to the paper's suggested procedure (b)

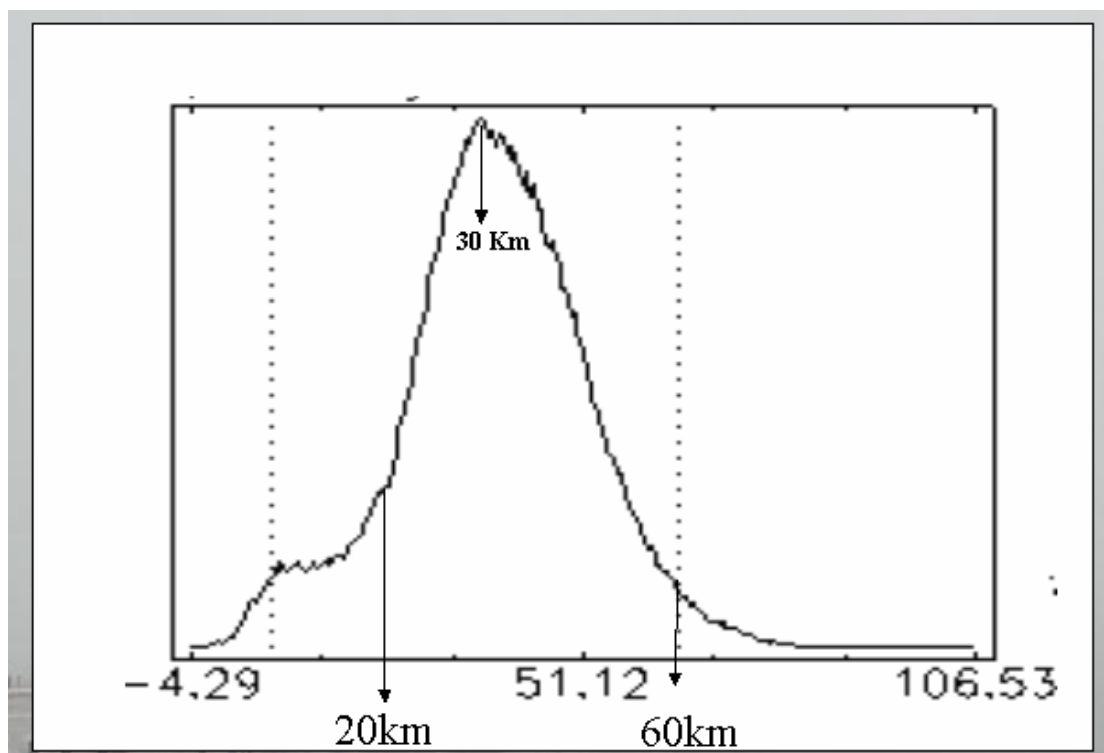


Figure 4: The histogram of the visibility image given in Figure 3a